Torque Control in Blended Antilock Braking Systems of Electric Vehicles

Valery Vodovozov, Eduard Petlenkov and Zoja Raud
Tallinn University of Technology
Tallinn, Estonia
valery.vodovozov@ttu.ee

Andrei Aksjonov
ŠKODA AUTO a.s.
Mladá Boleslav, Czech Republic
andrei.aksjonov@skoda-auto.cz

***Abstract*—The paper focuses on the braking torque control of road electric vehicles. Recommendations are issued regarding hierarchical system topology with torque allocation between electric and hydraulic brakes and the accurate accounting of the hybrid energy storage. Equally fast and safe braking is offered with maximal energy recovery on different roads, from dry to icy, without locking and skidding even in critical situations. Several parts of the system were explored in case studies that ensured their validity.**

Keywords— road electric vehicle; hybrid energy storage system; antilock braking system; blended braking system; fuzzy logic.

I. INTRODUCTION

New approaches are manifested now in the design of road electric vehicles (EV) fed by electrical drives (ED). Taking into consideration that from 15 to 50% of the urban driving energy is consumed by brakes [1], the electro-hydraulic blended braking systems are promoted nowadays [2] that envisage electric braking (EB), or recuperation, along with traditional hydraulic brakes (HB). Likewise, to promise energy recovery, hybrid energy storage (HES) combined the high energy density part (battery) and high power density part (ultracapacitors and/or flywheels) are promoted by several companies [3], [4]. Based on these trends, a new generation of blended antilock braking systems (ABS) arises that consolidate HB and EB features on the one hand with HES on the other hand.

Despite the potential advantages of the blended ABS, most of the EV braking control strategies primarily assign HB as the basic tool whereas the remaining part is supplemented by EB [5], [6]. In the case of high braking demand, the only HB is applied usually [7], [8]. While the requested braking strength is small, the HB works privately in some systems; though in [7] the solo EB plays the same role. Notably, that in the rear-wheel-drive EV the front wheels (FW) are usually supplied by HB solely whereas rear wheel (RW) torque is allocated between EB and HB [5], [9]. Conversely, in the front-wheel-drive EV, the RWs are fed by HB entirely and just FW torque is allocated between EB and HB [6]. When the high strength is requested, both FW and RW are provided with HB. As a result, recuperation is restricted in most of these cases. Only in the full-drive EV presented in [7], [10], [11], braking torque is distributed between FW and RW and allocated between EB and HB.

The most advanced ABS represent the slip-adjusted equipment [4], [5], [9] providing robust nonlinear vehicle slip tracking as the controlled variable. Part of them is referred to the fuzzy logic controller (FLC) [7] capable to discern successfully vague information about variable road surfaces, tire properties, and vehicle velocities. Unfortunately, they are valid only for specific bands of parameters being frequently "de-tuned" to accommodate worst-case scenarios, as it is difficult to establish fuzzy relations between all the variables based on intuition. In particular, in [10] the module for actuating braking torque calculation is composed of many rules regarding the brake pedal position, vehicle velocity, real-time torque, and battery state of charge (SOC). In [7], even without SOC, two outputs are generated by the FLC using an extensive rule base. In the similar manner, four inputs are processed into three outputs using a four-layer neural network in [4].

This study aims to demonstrate the HES-oriented blended ABS equally successful in both the gradual and the heavy braking situations under various operating conditions. To overcome tuning problems, the control action is shared here among three modules. The first one is the front-end block, which accurately processes input data. The second is the FLC for generating signals that cannot be calculated without expert estimates. The third is the algorithmic output stage, in which torque between FW and RW is distributed through a fixed ratio whereas torque between HB and EB is allocated based on the driver's setpoint and real-time SOC of power supply.

The research fits the hierarchical system topology [3], [11], [12] with ideal braking force distribution between FW and RW [7] according the ECE-R13 Regulation [13] followed the EV dynamics. The concern is to the car model and HES model clarifications as well as torque allocation. The objective is to analyse the effect of such features as energy recovery and system robustness to different road surfaces, providing vehicle handling with active recuperation keeping priority even in heavy braking situations, specifically with ABS.

978-1-5386-7312-6/18/$31.00 ©2018 IEEE

II. Braking Dynamics of Electric Vehicles

To slow down the EV from the initial velocity v by capturing vehicle energy W_B within the given time interval t, appropriate braking power P_B and force F_B have to be applied [2]:

$$W_B = \int P_B dt = \int F_B v dt \,. \tag{1}$$

In compliance with [2], [14], [15], dynamics of the decelerated vehicle are determined by

$$ma = F_B \tag{2}$$

where m is total EV mass and $a = -dv/dt$ – EV longitudinal deceleration.

The braking force of the EV is a combination of air friction F_{air}, climbing friction F_g, and rolling friction F_r [2]:

$$F_B = F_{air} + F_g + F_r. \tag{3}$$

Air resistance is given in [6], [10] as

$$F_{air} = 0.5\rho C_{air} Q \left(v \pm v_{wind}\right)^2 \tag{4}$$

where ρ is air density, C_{air} – aerodynamic drag coefficient, Q – EV front area, and v_{wind} – wind velocity.

The climbing force resists the EV to climb an incline:

$$F_g = mg \sin(\beta) \tag{5}$$

where g is acceleration due to gravity and β – climbing slope.

The rolling friction force

$$F_r = \mu\, mg \cos(\beta). \tag{6}$$

Here, μ is the tire-road friction factor (adhesive coefficient), the source of essential nonlinearity, time variability, and uncertainty of the braking dynamics.

To produce the braking force (2), appropriate braking torque T_B is calculated as the product of the braking force and the distance from the wheel axis at which it acts:

$$T_B = F_B r\,, \tag{7}$$

where r is the wheel effective radius. The corresponding power P_B of the braking system is as follows:

$$P_B = T_B \omega_w \tag{8}$$

where ω_w is the angular wheel speed.

Intensive braking causes longitudinal wheel slip λ [2], [11] as the relative motion of a wheel over the road:

$$\lambda = \frac{v - \omega_w r}{v}. \tag{9}$$

In [16], the adhesion-slip characteristics of the four-in-wheel-drives sport utility vehicle were found using the Pacejka's "magic formula" [14] and Automotive Simulation Models™ (ASM) interacted with MATLAB®/Simulink®. In Fig. 1, adhesion rises steeply from zero to its maximum between 0.05 and 0.15 slip. The rising slopes of the curves represent the stable zone while the falling slopes belong to the unstable zone where wheels may lock up and consequently induce skidding causing the wheel to spin.

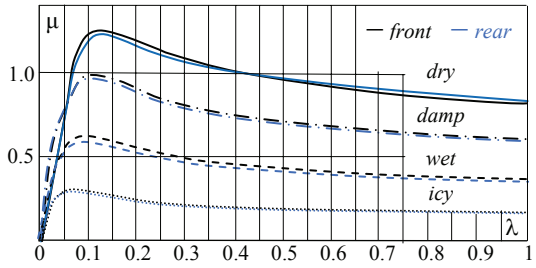

Fig. 1. Adhesive coefficient at different road surfaces.

Using (3) – (7), the stability condition may be formulated as follows:

$$\frac{d\mu}{d\lambda} \geq 0 \quad \text{or} \quad \frac{dT_B}{d\lambda} \geq 0 \tag{10}$$

III. The Model

The studied model of the EV braking (Fig. 2) contains four modules: Driver, Electronic Control Unit (ECU) with FLC, HES, and blended ABS containing EB and HB blocks.

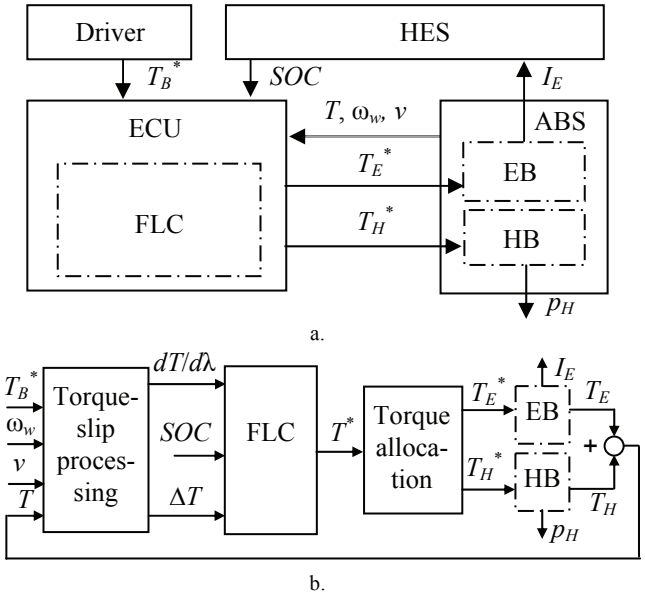

Fig. 2. The model of the EV braking system.

The braking sequence in Fig. 2 (a) is as follows. The driver judges the braking demand and treads the pedal according to the road conditions. Application braking force is produced by both the FW and RW. The ECU performs three functions:

- evaluation and conversion of the setpoint T_B^* to actuating braking torque T^*;
- distribution of actuating torque T^* between FW and RW based on the ideal power curve [4], [5], [7], [10], [11];
- allocation of actuating torque T^* between HB and EB.

Fig. 2 (b) explains ECU functionality. The system reads the pedal displacement signal of driver's setpoint T_B^*, the real-time feedback signals, such as application torque T from either the torque sensors or the direct torque control system (DTC), angular wheel speeds ω_w, EV velocity v from either the GPS or acceleration sensors, and SOC signals from HES.

Using this information, ECU calculates longitudinal wheel slip λ, the derivative $dT/d\lambda$ of real-time application torque with respect to slip, and actuating braking torque T^* for further distribution and allocation. From ECU, the EB and HB torque commands T_E^*, T_H^* go to appropriate ABS inputs. The current I_E recharges HES from EB whereas pressure p_H adjusts the HB. Braking ends as the pedal is released or the vehicle stops.

At normal EV design, the maximal power $P_{ED\max}$ that ED develops during slowing down or downhill movement meets the traction power (8) at the maximal velocity and adhesion $\mu < 0.1$. At gradual braking, the required adhesive coefficient may overcome this level, whereas at heavy braking, the adhesive coefficient increases rapidly approaching 1.

To allocate actuating torque T^* between EB and HB, the ED is considered as capable to charge either of HES parts:

$$\begin{aligned} P_{ED\max} &> \{P_{UC\max} \vee P_{BAT\max}\} \\ U_{ED\max} &> \{U_{UC\max} \vee U_{BAT\max}\} \\ I_{ED\max} &> \{I_{UC\max} \vee I_{BAT\max}\} \end{aligned} \quad (11)$$

where $P_{UC\max}$, $U_{UC\max}$, $I_{UC\max}$, $P_{BAT\max}$, $U_{BAT\max}$, $I_{BAT\max}$ are maximal power, voltage, and current of the ultracapacitor and the battery, respectively; $U_{ED\max}$, $I_{ED\max}$ – maximal voltage and current of the ED; $\vee$ – maximum operator.

On the other hand, to keep the ultracapacitor and the battery inside the safe margins at any instant, ED torque T_E^* and current I_E have to be limited by the real-time HES conditions, namely, SOC_{UC} and SOC_{BAT} [4]:

$$T_E^* = I_E\psi = \{I_{UC}(SOC_{UC})\psi \vee I_{BAT}(SOC_{BAT})\psi\} \quad (12)$$

where I_{UC}, and I_{BAT} are the real-time recharging currents of the ultracapacitor and battery and ψ is the ED flux linkage.

The remaining fraction of actuating braking torque is requested from the HB:

$$T_H^* = T^* - T_E^*. \quad (13)$$

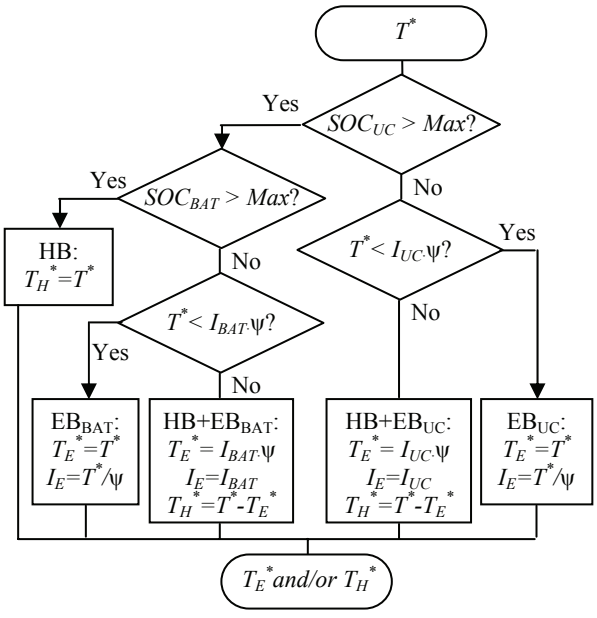

Fig. 3. Flowchart of braking torque allocation.

where desired HB torque relates to HB pressure p_H and HB coefficient k_H as follows:

$$p_H = k_H \cdot T_H^* \quad (14)$$

Fig. 3 demonstrates the appropriate torque allocation strategy. Here, the sole HB is used only while both *SOC* levels overcome permissible overcharging barriers (*Max*) due to recuperation impossibility. Since one or both *SOCs* drop, EB_{UC} or EB_{BAT} comes into play being active alone until ED torque becomes insufficient to maintain actuating torque T^*. In the latter case, conventional for ABS, the ECU runs both HB and EB (HB+EB_{UC} or HB+EB_{BAT}). A particular strength of this strategy is the ability to use EB in most situations, including heavy braking.

IV. FLC Design and Simulation

The FLC design was conducted in LabVIEW®. To determine actuating braking torque required to slowdown the EV within an acceptable adhesion-slip region, two input numerical variables (crisps) and one output were introduced: application real-time torque T and torque derivative $dT/d\lambda$ with respect to slip, and actuating torque T^*. Using the Mamdani's inference mechanism [17], every crisp was translated by the FLC into a fuzzy set, which, in turn, unites an element in universe of discourse (UOD) and a degree of membership function (MF). The output is then turned back to the real world by the centre-of-gravity defuzzification method.

The input and output variables have the closed frontiers of their UODs. The torque T input, torque derivative $dT/d\lambda$ input, and actuating torque T^* output with UOD restrictions narrowed in [0, 10000 Nm] have four MFs notated as Z (Zero), S (Small), M (Middle), and L (Large). Fig. 4 represents the fuzzy sets for the input linguistic variables those MFs have triangle and trapezoidal shapes that are enough accurate for control and easy for expert's training.

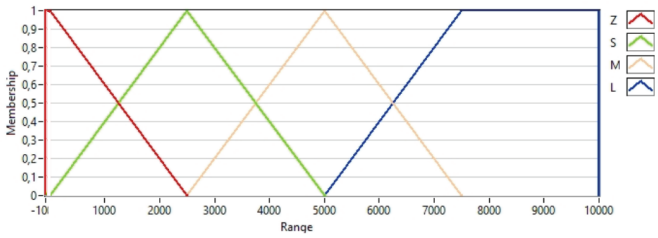

Fig. 4. MFs of control variables T, $dT/d\lambda$, and T^*.

The rule base stores the linguistic knowledge needed for converting the fuzzy input sets into the fuzzy output set by the inference engine. Using "If–Then" modus ponens, the rule base of 16 rules has been developed (Table I).

TABLE I. FLC Rule Base

Torque derivative $dT/d\lambda$	Output torque T^* at input T			
	Z	***S***	***M***	***L***
Z	Z	Z	Z	Z
S	Z	S	S	S
M	Z	S	M	M
L	Z	M	M	L

An appropriate three-dimensional surface (T- $dT/d\lambda$- T^*) is represented in Fig. 5.

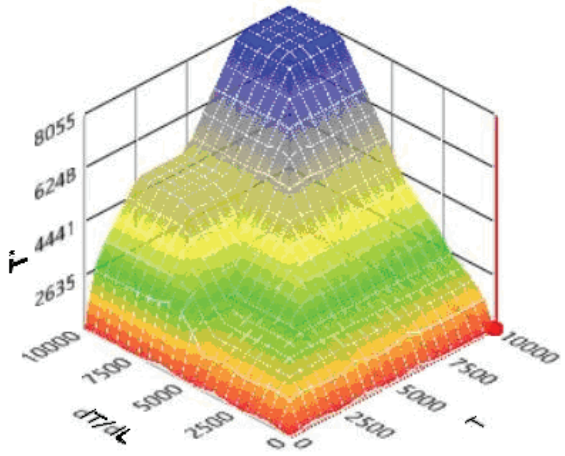

Fig. 5. ABS FLC surface

Electro-mechanical simulation was conducted in eDrive® for the sport utility vehicle with m=2117 kg, Q=3 m^2, μ=0.01, r=0.2 m, ρ=1.2 kg/m^3, C_{air}=0.5, β = 0, and gear ratio=10.5. To run at v = 100 km/h, 25 kW power and 180 Nm torque were applied. Braking processes shown in Fig. 6 were simulated for switch-reluctance motor of P_{nom}=42 kW, $T_{\max}$ = 200 Nm, and U_{BAT}=400 V. DTC was implemented using cascading current-speed PID controllers with modulus optimum settings [18]. In Fig. 6 (a), only EB was used, without HB. Braking began from the first second and proceeds, at its best, 100 ms at ABS frequency 100 Hz. However, to provide braking with μ=1, the ABS demands T_B = 4300 Nm instead of 200 Nm. It means, the remaining 4100 Nm is to be obtained from HB. As Fig. 6 (b) shows, the braking time of blended braking drops threefold.

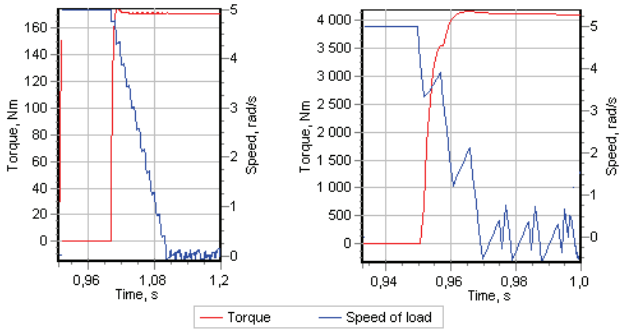

a. b.

Fig. 6. EB without HB (a) and braking in blended ABS (b)

V. Conclusion

The model of the EV braking process was designed and studied in this paper. It provides evaluation and conversion of the setpoint to actuating braking torque, distribution of actuating torque between FW and RW, and allocation of actuating torque between HB and EB. The fuzzy ABS designed adjusts braking torque and slip within about 6 ms, before the wheel can lock with energy recovering. Herewith, while the setpoint braking torque can be sufficiently supplied by the EB system, the solo ED is used. Otherwise, both EB and HB share the required braking strength. Independent HB is applied only in the case of recuperation impossibility.

Acknowledgment

This study has received partial funding from the European Union's Horizon 2020 research and innovation program under grant agreement No. 675999.

References

[1] S. M. Savaresi and M. Tanelli, Active Braking Control Systems Design for Vehicles, London: Springer, 2010, 254 p.

[2] Brakes, Brake Control and Driver Assistance Systems: Function, Regulation and Components, K. Reif (Ed.), Friedrichshafen, Germany: Springer, 2014, 275 p.

[3] J. Peng, H. He, W. Liu and H. Guo, "Hierarchical control strategy for the cooperative braking system of electric vehicle," Scientific World Journal, vol. 2015, no. 4, 2015, pp. 1 – 11.

[4] F. Naseri, E. Farjah and T. Ghanbari, "An efficient regenerative braking system based on battery/supercapacitor for electric, hybrid, and plug-in hybrid electric vehicles with BLDC motor," IEEE Transactions on Vehicular Technology, vol 66, no 5, pp. 3724 – 3738, May 2017.

[5] Z. Chen, T. Lv, N. Guo, J. Shen, R. Xiao, X. Lu and Z. Yu, "Study on braking energy recovery efficiency of electric vehicles equipped with super capacitor," Chinese Automation Congress (CAC), Jinan, China, 2017, pp. 7231 – 7236.

[6] D. Zhu, X. Wang, Y. Li and Y. Wang, "Research on energy regenerative braking of electric vehicle based on functional safety analysis," 2nd Asia-Pacific Conference on Intelligent Robot Systems (ACIRS), Singapore, 2017, pp. 326 – 330.

[7] Y. Wang and Y. Su, "A research for brake strategy based on fuzzy control in pure electric vehicles," 4th International Conference on Computer Science and Network Technology (ICCSNT), Harbin, China, 2015, pp. 689 – 693.

[8] A. Dadashnialehi, A. Bab-Hadiashar, Z. Cao and A. Kapoor, "Intelligent sensorless antilock braking system for brushless in-wheel electric vehicles," IEEE Transactions on Industrial Electronics, vol. 62, no. 3, pp. 1629 – 1638, March 2015.

[9] J. Dou, G. Cui, S. Li, X. Zhao, X. Lu and Z. Yu, "MPC-based cooperative braking control for rear-wheel-drive electric vehicle," Chinese Automation Congress (CAC), Jinan, China, 2017, pp. 4419 – 4424.

[10] Y. Tao, X. Xie, H. Zhao, W. Xu and H. Chen, "A regenerative braking system for electric vehicle with four in-wheel motors based on fuzzy control," 36th Chinese Control Conference (CCC), Dalian, China, 2017, pp. 4288 – 4293.

[11] P. Spichartz, T. Bokker and C. Sourkounis, "Comparison of electric vehicles with single drive and four wheel drive system concerning regenerative braking," 12th International Conference on Ecological Vehicles and Renewable Energies (EVER), Monte-Carlo, Monaco, 2017, pp. 1 – 7.

[12] C. Satzger and R. De Castro, "Predictive brake control for electric vehicles," IEEE Transactions on vehicular technology, vol. 67, no. 2, pp. 977 – 990, February 2018.

[13] Regulation No. 13-H of the Economic Commission for Europe of the United Nations (UN/ECE) — Uniform provisions concerning the approval of passenger cars with regard to braking, 2015/2364.

[14] H. B. Pacejka, Tyre and Vehicle Dynamics, Oxford, UK: Butterworth−Heinemann, 2006, 672 p.

[15] M. Ehsani, Y. Gao and A. Emadi, Modern Electric, Hybrid Electric, and Fuel Cell Vehicles: Fundamentals, Theory, and Design, London: CRC Press, 2010, 534 p.

[16] A. Aksjonov, K. Augsburg and V. Vodovozov, "Design and simulation of the robust ABS and ESP fuzzy logic controller on the complex braking maneuvers," Applied Sciences, vol. 6, no. 12, 2016, pp. 382 – 390.

[17] M. Negnevitsky, Artificial Intelligence: A Guide to Intelligent Systems, Harlow, UK: Addison-Wesley, 2005, 435 p.

[18] V. Vodovozov, Electrical Drive: Performance, Design and Control, Saarbrücken, Germany: LAP, 2014, 320 p.